Team Number :	apmcm2101225
Problem Chosen :	B

The Optimal Design of Thermal Emitter in Thermophotovoltaic Technology Based on Particle Swarm Optimization

Firstly, when studying the relationship between emission spectra of single-layer structure and material properties, the **Transfer Matrix Method** is used to calculate the emission spectra.At the same time, the **Fresnel coefficient** is introduced to represent the emission spectrum of the thermal radiator, and the model of the emission spectrum and material properties of the single layer structure thermal radiator is established to represent the relationship between the emission spectrum of the single layer and the material properties. The **emission spectrum** of **50 nm** thick tungsten in the range of 0.3-50 micron is calculated to be **0.03-0.48(λ T)**, and the emission spectrum is given in the following. Finally, through the **model test** of tungsten with different thicknesses, it is found that the emission spectra of tungsten with different thicknesses have similar trends, so the correctness of the model is proved.

Secondly,the **complex-amplitude reflection** and **transmission coefficient** between multilayer materials are taken into account. Combined with the **Matrix Transfer Method** of problem 1, the Fresnel coefficient of the double-layer structure is calculated, and the emission spectrum and material properties model of the **double-layer structure** is obtained. Finally, the double-layer structure is **mathematically generalized**, and the relationship model between the emission spectrum and material properties of the **multi-layer structure** is obtained. The composite emission spectra of 50 nm thick tungsten and silicon dioxide were calculated to be **0.02 – 0.39 (λ T)** in the range of 0.3 – 50 microns, and the emission spectra were given below.

Thirdly, in order to improve the spectral control ability of the thermal emitter, the **material informatics** method of alternating **Bayesian optimization.** A **Q factor** which can indirectly represent the spectral radiance of the thermal emitter is introduced as an **auxiliary parameter** of the Bayesian optimizer. Finally, the number of layers of the emitter, the type of material per layer, the thickness of each layer (micron) and the Q factor can be **(9, {Ge, Y2O3, Ge, Y2O3, Ge, Y2O3, Ge, SiO2, W}, 3.85, 192)**.

Finally, the **particle swarm optimization algorithm** is used to solve the corresponding problem. The design parameters of the corresponding heat emitter are calculated as **(8, {Y2O3, Ge, SiO2, Ge, Y2O3, Ge, SiO2,GaSb},3.85, 204)**.Finally, the design parameters of the emitter are **(8, {SiO2, Ge, SiO2, Ge, SiO2, Ge, SiO2, GaSb}, 3.81, 204)**, and the error between **the numerical value** and the original model value is **within 7.2 %**.

Keywords: Matrix transfer method; Bayesian ptimization; Materials informatics;
The thermal emitter model based on particle swarm optimization

Contents

1. Introduction

1.1. Problem Background

In recent years, various space exploration programmes have been developed around the world. 2021 saw the completion of the expected mission of the China's "Zhu Rong", which is still on Mars, searching for more new discoveries in the universe. Thermophotovoltaic technology uses various heat sources to heat the thermal emitters and converts the infrared radiation from the thermal emitters into electrical energy via photovoltaic cells. Thereby, thermophotovoltaic technology ensures that various instruments and equipment can function without sunlight.

Photovoltaic cells primarily convert high-energy photons below a specific band-gap wavelength. Thermal emitters mainly use different material structures to regulate the emission of the absorbed heat so that most of the emitted photons are below the bandgap wavelength of the photovoltaic cell. As the low-energy photons above the wavelengths absorbed by the cell cannot be converted into electricity by the photovoltaic effect, the photoelectric conversion efficiency of the cell is reduced. Therefore, in order to improve the thermoelectric conversion efficiency of the thermophotovoltaic system, the emission spectrum of the thermal emitter must be adjusted. The main methods for calculating the emission spectrum include the Transfer Matrix Method (TMM) [1-2], the Finite Difference Time Domain Method (FDTD), and the Rigorous Coupled Wave Analysis Method (RCWA). The main factors affecting the emission spectrum of a thermal emitter are the optical properties (refractive index or dielectric constant) and structural properties (thickness) of the material.

1.2. Restatement of the Problem

Problem 1: Please describe the relationship between the emission spectra of single-layer structure and the material properties, including refractive index and thickness, and calculate the emission spectrum of 50 nm thick tungsten in 0.3-5 microns.

Problem 2: Please indicate the relationship between the emission spectra of the multilayer structure and the material properties, including refractive index and thickness, and calculate the emission spectrum of the composite structure formed by 50 nm tungsten and 50 nm silicon within 0.3 to 5 microns.

Problem 3: The narrow-band design of thermal radiator can concentrate the emission wavelength in a very small range, so as to improve the thermoelectric conversion efficiency of thermal power plant. Design a multiplayer thermal emitter to be as narrow and high as possible, parameters (the number of layers, the material, thickness of each layer) and its emission spectrum.

Problem 4: Assume that the band-gap wavelength of GaSb cell is 1.71 microns. The emission spectrum of its idealized heat emitter is given in the original text. The blue dots and lines on the figure show the external quantum efficiency, whose effects can be appropriately considered. Please select materials to design a multilayer thermal emitter for GaSb battery to achieve the highest thermoelectric conversion efficiency, and give the design parameters of multilayer structure and its emission spectrum.

2. Problem analysis

2.1. Problem one analysis

In response to problem one in the study of the relationship between the emission spectra of single-layer structures and material properties, this article uses the Transfer Matrix Method for the calculation of the emission spectra. For metals of interest such as tungsten, electromagnetic radiation effects are largely determined by the free conduction electrons received in the metal. Therefore, the Drude model can give a simple representation of the out-of-phase oscillations of the free electrons in the electric field. The article also takes into account the fact that metals have a negative buffer constant at optical frequencies, which has a large effect on the reflectivity of the metal. The two different types of waves are represented by introducing the Fresnel coefficient. Based on the description above, the relationship between the emission spectra of the single-layer structure and the material properties can be expressed and values can also be calculated for 50 nm thick tungsten in the range 0.3-5 μm.

2.2. Problem two analysis

For wave radiation in general, the optical reflectance and transmittance of a multilayer structure material can be expressed by the product of matrices. In this article, it is reasonable to assume that this multilayer material is a multilayer parallel structure which is isotropic in its optical properties and consists of uniform layers. The elements transferred by the multiplication of the matrices are represented by the complex-amplitude reflection and the transmission coefficients r and t, respectively. This question firstly requires analysis of the two-layer material for the multilayer structure material. The complex-amplitude reflection and transmission of the two-layer material shoule be expressed in this model. The relationship between the emission spectra of the two-layer structure and the material properties and finally obtained by the Fresnel coefficient in combination with the matrix transfer method of the first problem. Finally the model could be generalized to apply to the emission spectra and material properties of multilayer structures.

2.3. Problem three analysis

In problem three, in order to improve the spectral control of the emitter so that the emission spectrum of the thermal emitter is concentrated in a very small wavelength band, the design of a thermal emitter with a multilayer structure can be developed by means of a material informatics approach alternating Bayesian optimisation and thermal electromagnetic field calculations. The objective function is the maximum thermal spectral emission, the maximum value of which is set near the wavelength of 1.5 μm according to the title. Finally, using machine learning methods, the number of layers of the multilayer structured thermal emitter, the material used in each layer and the type of material are trained as parameters. What is more, a Q-factor, which can indirectly represent the spectral radiation of the thermal emitter, is introduced as an auxiliary parameter.

2.4. Problem four analysis

The problem requires the design of a multilayer emitter for a GaSb cell to achieve the highest possible thermoelectric conversion efficiency. The band gap wavelength of GaSb is known to be 1.71 μm and the question gives the external quantum efficiency (EQE) to assist in checking the validity of the model. This problem can first be based on

the model of a multilayer structured thermal emitter established in Problem 3, which can be improved by changing the interval where its maximum value lies from 1.5 μm to 1.71 μm, while introducing the thermoelectric conversion efficiency as the objective function value. A particle swarm algorithm is considered to solve the modified multilayer structure heat emitter model to obtain the design parameters of the multilayer structure. Finally a model check should be carried out to add the exo-quantum efficiency to the multilayer structural heat emitter model so that the results obtained are compared with those without the exo-quantum efficiency and to check the correctness of the model.

3. Assumptions

a. The phase oscillation of the free electrons in the metal in the electric field is stable and can be described by a model.
b. The electromagnetic waves radiated by the thermal emitter are stable in the orthogonal direction and do not affect each other in phase.
c. The complex amplitude reflection and projection coefficients between different layers of material can be measured and are specified as constant values.
d. The design parameters of the thermal emitter do not change due to the space environment and are specified as constant values.

4. Notations

The key mathematical notations used in this paper are listed in Table 1.

Table 1: Notations used in this paper

Symbol	Description
E_i	Energy of the ith object
n_i	Snell's constant of the ith object
θ_i	Angle of incidence of object i
r_i	refractive index of object i
t_i	Transmittance of object i
A_l	Amplitude of the forward wave of the thermal emitter
B_l	Amplitude of the backward traveling wave of the thermal emitter
$d_{(l)}$	Thickness of the lth layer of the thermal emitter
$\gamma_{(l)}$	Emission spectrum of the material in layer l
P_l	Propagation matrix of materials adjacent to layer l
σ_l	Radiation loss penalty factor for layer l

5. Establishment and Solution of Model

5.1. Model and solution of problem one

To investigate the relationship between the emission spectra of single-layer structures and material properties , it should first be considered that the electromagnetic radiation effect received by single-layer metal structures is largely determined by the free conduction electrons in the metal. Besides, the special optical properties of metal structures, such as the negative buffering constant of metals at optical frequencies, lead to very high reflectivity.

Furthermore, considering that in optical frequencies, the free metal electron gas can sustain oscillations in surface and bulk charge density, plasma polaritons and plasma have different resonant frequencies[1]. Thus when an electromagnetic wave falls on a metal surface, it produces optical interference between two symmetric regions and splits into two waves. The first one is a falling wave close to the optical interference called Transmitted wave T and the second one is called Reflected wave R.

Two types of polarization are produced, depending on the angle of the wave falling on the surface of the metallic material. One is parallel polarization. Two electromagnetic fields are produced when the electromagnetic wave falls, the electric field in the x direction on the surface of the metallic material and the magnetic field in the y direction perpendicular to the surface of the material and moving laterally in the z direction. The other one is vertical polarization[2]. The electric field is perpendicular to the surface of the metallic material in the y-direction, moving laterally in the z-direction, and the magnetic field is perpendicular to the material surface in the x-direction. Finally, the amount of electromagnetic wave remaining after passing through the metal material can be measured according to the wave propagation detection damage method to produce the transparent bond value, and the spectrum emitted by the metal material is calculated by the Tranfer Matrix Method (TMM) to derive the expression.

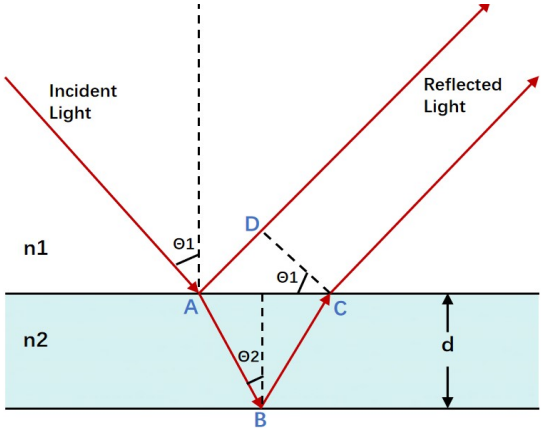

Figure 1: Schematic of Matrix Transfer Method

5.1.1. Propagation equation of electromagnetic wave

To illustrate the propagation equations of electromagnetic waves, the fundamental Maxwell's equations , which are expressed as follows, should be introduced first:

$$\varepsilon_1 E_1^{\perp} = \varepsilon_2 E_2^{\perp} \quad (1)$$

$$B_1^{\perp} = B_2^{\perp} \quad (2)$$

$$E_1^{\parallel} = E_2^{\parallel} \quad (3)$$

$$\frac{B_1^{||}}{\mu_1} = \frac{B_2^{||}}{\mu_2} \tag{4}$$

In addition, Snell's law of refraction is:

$$n_1 sin\theta_1 = n_2 sin\theta_2 \tag{5}$$

According to the relationship between angle of incidence of the wave for metallic materials as above mentioned and the condition that the electric field is vertical (Es) and parallel[3] (Ep), the Fresnel constants can be arrived at with Equation(3) and (4), which are expressed as follows:

$$r_s = \frac{E_{r,s}}{E_{i,s}} = \frac{n_1 cos\theta_1 - n_2 cos\theta_2}{n_1 cos\theta_1 + n_2 cos\theta_2} \tag{6}$$

$$t_s = \frac{E_{t,s}}{E_{i,s}} = \frac{2n_1 cos\theta_1}{n_1 cos\theta_1 + n_2 cos\theta_2} \tag{7}$$

$$r_p = \frac{E_{r,p}}{E_{i,p}} = \frac{n_2 cos\theta_1 - n_1 cos\theta_2}{n_2 cos\theta_1 + n_1 cos\theta_2} \tag{8}$$

$$t_p = \frac{E_{t,p}}{E_{i,p}} = \frac{2n_1 cos\theta_1}{n_2 cos\theta_1 + n_1 cos\theta_2} \tag{9}$$

The propagation equation of electromagnetic wave can be obtained through the equation above and shown as follows:

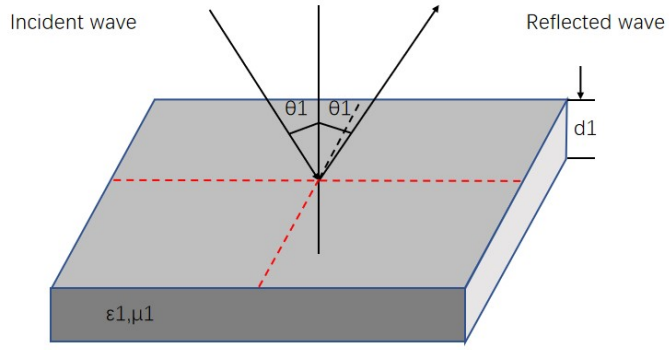

Figure 2: Schematic diagram of electromagnetic wave propagation

5.1.2. Representation of the Transfer Matrix Method (TMM)

For the study of the emission spectra of single-layer materials, first of all, this article expresses the refractive index of the material in the x,y,z direction from the material with the equation:

$$\varepsilon_1 = \begin{cases} \varepsilon_1, 0 < z < d_1 \\ \varepsilon_2, d_1 < z < d_2 \end{cases} \tag{10}$$

$$\varepsilon_{1(z)} = \varepsilon_{l(z+d)} \tag{11}$$

L is the number of layers of the material (1 for a single-layer structure at here) and d is the period of the wave in figure 1.

In this paper, based on Maxwell's equations and boundary conditions, the emission spectra of single-layer materials are decomposed from the x, y, and z directions using

matrix transfer methods to obtain TM polarization values and TE polarization values, respectively[4].

The specific expression for the TM polarization value is:

$$H_{ly} = A_l e^{if(x,\theta,z)} + B_l e^{ig(x,\theta,z)} \tag{12}$$

$$E_{lx} = \eta_l cos\theta_l (A_l e^{if(x,\theta,z)} - B_l e^{ig(x,\theta,z)}) \tag{13}$$

$$E_{lx} = -\eta_l cos\theta_l (A_l e^{if(x,\theta,z)} + B_l e^{ig(x,\theta,z)}) \tag{14}$$

Where A_l is the amplitude of the forward wave, and B_l is the amplitude of the trailing wave.

The specific expression for the TE polarization value is as follows:

$$E_{ly} = A_l e^{if(x,\theta,z)} + B_l e^{ig(x,\theta,z)} \tag{15}$$

$$E_{lx} = \frac{\eta_l}{cos\theta_l} (A_l e^{if(x,\theta,z)} - B_l e^{ig(x,\theta,z)}) \tag{16}$$

$$E_{lx} = \frac{\eta_l}{cos\theta_l} (A_l e^{if(x,\theta,z)} + B_l e^{ig(x,\theta,z)}) \tag{17}$$

The expressions for the simultaneous wave number and the intrinsic barrier are as follows:

$$K_l = w\sqrt{\varepsilon_0 \mu_0 \varepsilon_1 \mu_1} \tag{18}$$

$$\eta_l = \frac{k_l}{w\varepsilon_0 \varepsilon_1} \tag{19}$$

5.1.3. Modeling of the emission spectra of single-layer structures

For the electromagnetic wave propagation equation and matrix transfer method given above, this paper matrixes the equation by using the boundary conditions and the E domains H domains conditions.

$$\begin{bmatrix} E_1 \\ H_1 \end{bmatrix} = M_1 M_2 \dots M_{l-1} M \begin{bmatrix} E_l \\ H_l \end{bmatrix} \tag{20}$$

The specific expressions for M_i ,i=1,... l-1, are as follows:

$$M_{(l-1)} = \begin{bmatrix} cos\delta & i\gamma sin\delta \\ i\gamma^{-1} sin\delta & cos\delta \end{bmatrix} \tag{21}$$

Based on the description above, the relationship between emission spectrum of single-layer material, incident Angle of wave, optical constant and material thickness can be obtained as follows:

$$\gamma_{(l-1)} = k_{(l-1)} d_{(l-1)} cos\theta_{(l-1)} \tag{22}$$

Also the relationship between the angle of incidence and the refractive index is expressed using the Snell's law of refraction[5], which is given by Equation (5).

Therefore, the relationship between the emission spectra of single-layer structures and material properties is modeled as follows.

$$\gamma_{(l-1)} = k_{(l-1)} d_{(l-1)} cos(arcsin \frac{n_{(l-1)} sin\theta_{(l-1)}}{n_l}) \tag{22}$$

Where $\gamma_{(l-1)}$ is the emission spectrum of the single-layer material, $d_{(l-1)}$ is the

thickness of the single-layer material, and $\theta_{(l-1)}$is the angle of incidence.

5.1.4. Analysis of results

In this paper, the above equation is calculated by MATLAB software for a tungsten thickness of 50 nm, i.e.$d_i = 50nm$, put into Equation (22). The emission spectra of 50 nm thick tungsten in the range of 0.3-50 μm are calculated by the relevant code of the electromagnetic wave propagation equation and matrix transfer method as follows[6].

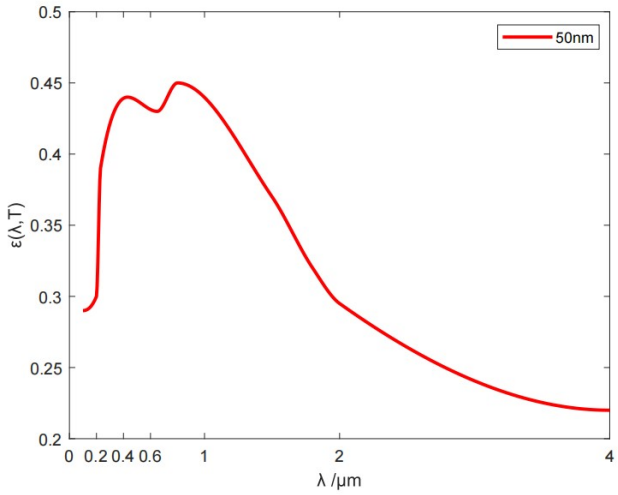

Figure 3: Emission Spectra of 50nm Tungsten

The model was tested by substituting the values for different thicknesses of tungsten into the equation and the following emission spectra were obtained.

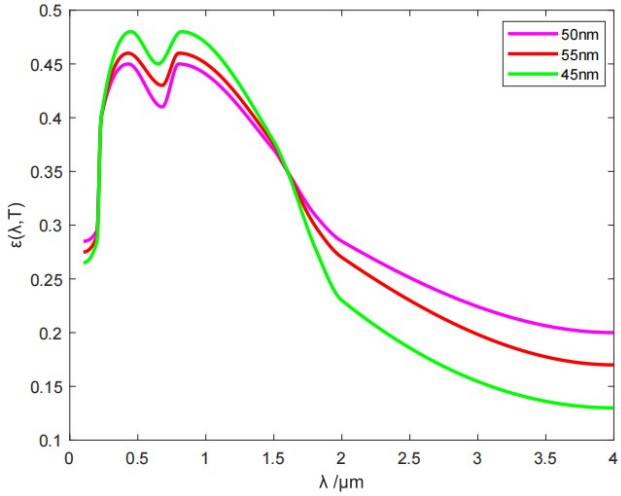

Figure 4: Emission Spectra of Tungsten with Different Thickness

The figure show that the trend of the emission spectra is similar for different thicknesses of tungsten to some extent, in accordance with the studies in the literature on the subject[7]. Therefore, it is considered that the model established in this problem for the emission spectra of single-layer materials and material properties is correct.

5.2. Model and solution of problem two

For wave radiation in the general case, the optical reflectance and transmittance of a multilayered structural material can be represented accordingly by the product of matrices[8]. The assumption of coherent light propagation, which is implicit in multilayered structural materials in the usual sense, may lead to oscillations in the calculated values of reflectance and emission spectra. And the above oscillations occur when one layer of the multilayer structure is thick enough and transparent enough to produce multiple coherent reflections[9]. Therefore, in this paper, when modeling the relationship between the emission spectra and material properties of multilayer structures, the two-layer structure is first considered. Then the established model is generalized to finally obtain the relationship between the emission spectra of multilayer structures and material properties.

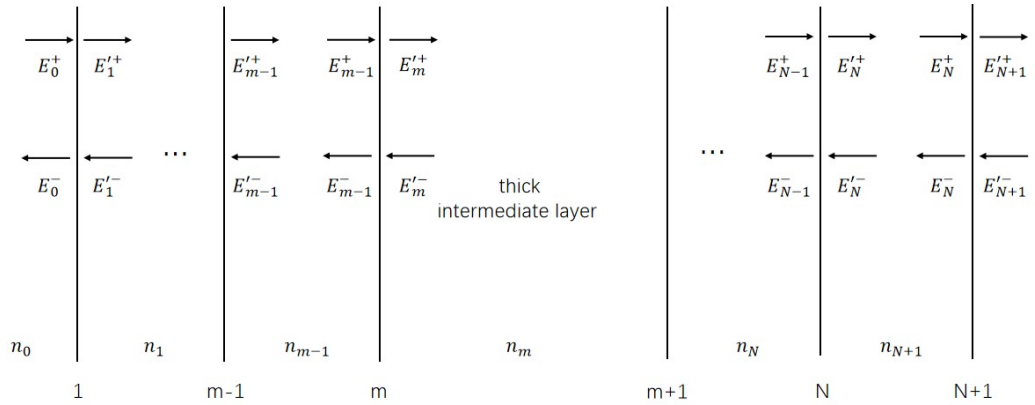

Fugure 5: Diagram of multilayer structure thermal emitter

5.2.1. Systematic transmission matrix representation of the emission spectrum

For a two-layer structure, waves on the left and right sides of each layer of the structure[10], whose amplitudes and projection coefficients on each side can be represented by a two-dimensional matrix with the following expressions, are considered in this article.

$$\begin{pmatrix} E_1^+ \\ E_1^- \end{pmatrix} = D_1^{-1} D_2 \begin{pmatrix} E_2^{'+} \\ E_2^{'-} \end{pmatrix} \tag{23}$$

The D_1, D_2 are the kinetic matrix of 2×2. E_1, E_2 are the amplitudes and projection coefficients of the electromagnetic waves on the left and right sides of each layer of the structure.

In addition, the expression for the kinetic matrix multiplication $\mathrm{D}_1^{-1}\mathrm{D}_2$ is:

$$\mathrm{D}_1^{-1}\mathrm{D}_2 = \frac{1}{\mathrm{t}_{\mathrm{m-1,m}}} \begin{bmatrix} 1 & \mathrm{r}_{\mathrm{m-1,m}} \\ \mathrm{r}_{\mathrm{m-1,m}} & 1 \end{bmatrix} \tag{24}$$

Also considering the refractive index and thickness of the two-layer structure, the operation of matrix product has the expression:

$$\begin{pmatrix} \mathrm{E}_1^+ \\ \mathrm{E}_1^- \end{pmatrix} = \mathrm{D}_1^{-1}\mathrm{D}_1\mathrm{P}_0\mathrm{D}_2^{-1}\mathrm{D}_2 \begin{pmatrix} \mathrm{E}_2^{'+} \\ \mathrm{E}_2^{'-} \end{pmatrix} \tag{25}$$

where P_0 is the propagation matrix of the two-layer material system, the D_1 and

$D_2$are the kinetic matrices.

By describing the above equations, the transmission matrix T of the system with a two-layer structure is obtained, and its specific expressions are:

$$T = \begin{bmatrix} T_{11} & T_{12} \\ T_{21} & T_{22} \end{bmatrix} = D_1^{-1} D_1 P_0 D_2^{-1} D_2 \tag{26}$$

5.2.2. Decomposition of the transmission matrix of a two-layer architecture system

For the system transmission matrix given in the first part, this article decomposes it to obtain the reflectance and transmittance of the two layers of the two layers of the matrix, respectively, whose specific expressions are:

$$r = \frac{E_1^-}{E_1^+}(E_2'^- = 0) = \frac{T_{21}}{T_{11}} \tag{27}$$

$$t = \frac{E_2'^+}{E_1^+}(E_2'^- = 0) = \frac{1}{T_{11}} \tag{28}$$

$$r' = \frac{E_1^-}{E_2^+}(E_1^+ = 0) = -\frac{T_{12}}{T_{11}} \tag{29}$$

$$t' = \frac{E_0^-}{E_2^+}(E_1^+ = 0) = \frac{\mathrm{Det}\, T}{T_{11}} \tag{30}$$

Where $r, t, r', \text{and } t'$ denote the reflectance and transmittance of the left and right sides of the two-layer structure, respectively.

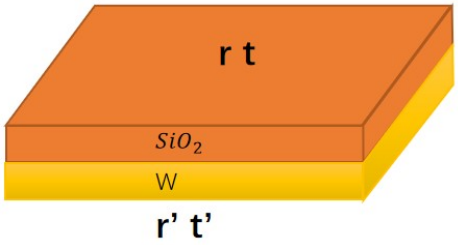

Figure 6: Diagrams of reflectivity and transmittance of different materials

Det is the determinant of the system transfer matrix, specified by the expression:

$$Det\, T = T_{11}T_{22} - T_{12}T_{21} \tag{31}$$

Then equation (26) is updated according to equations (27), (28), (29), (30), and the specific expression is:

$$T = \begin{bmatrix} T_{11} & T_{12} \\ T_{21} & T_{22} \end{bmatrix} = \frac{1}{t}\begin{bmatrix} 1 & -r \\ r & tt' - rr' \end{bmatrix} \tag{32}$$

5.2.3. Modeling of emission spectra and material properties of two-layer structures

By the above equation, in the two-layer structure, the absorption of electromagnetic waves occurs at the intersection of the spectra out of different substances, and at the same time, it will have an effect on the phase difference between the reflected and projected beams[11]. So the above-mentioned reflectance and transmittance are corrected here, and the correction results are as follows:

$$r_{new} = r_{old}e^{-2(sn_1\sigma)^2} = \alpha r_{old} \tag{33}$$

$$r'_{new} = r'_{old}e^{-2(sn_2\sigma)^2} = \beta r'_{old} \tag{34}$$

$$t_{new} = t_{old}e^{-\frac{1}{2}(s\sigma)^2(n_2-n_1)^2} = \gamma t_{old} \tag{35}$$

$$t'_{new} = t'_{old}e^{-\frac{1}{2}(s\sigma)^2(n_1-n_2)^2} = \gamma t'_{old} \tag{36}$$

With the above modified equations, the reflectance and transmittance at the intersection of different materials in the two-layer structure are expressed in this paper as follows:

$$R = r_0^2 + \frac{|t_1 t_2 r_1|^2 e^{-4\frac{\sigma}{c}k_1 d_1}}{1 - |r_1 r_2|^2 e^{-4\frac{\sigma}{c}k_1 d_1}} \tag{37}$$

$$T = t_0^2 + \frac{|t_2|^2 e^{-2\frac{\sigma}{c}k_1 d_1}}{1 - |r_1 r_2|^2 e^{-4\frac{\sigma}{c}k_1 d_1}} \tag{38}$$

For the corrected reflectance and transmittance, and in conjunction with the electromagnetic wave propagation equations given above and the matrix transfer method[12], the above equations are matrixed as follows:

$$\begin{bmatrix} r_1 & r_2 \\ t_1 & t_2 \end{bmatrix} = T_1 T_2 \begin{bmatrix} r'_1 & r'_2 \\ t'_1 & t'_2 \end{bmatrix} \tag{39}$$

Where T_i ,i=1,2 the specific expressions are as follows:

$$T_i = \begin{bmatrix} T_{11} & T_{12} \\ T_{21} & T_{22} \end{bmatrix} = \frac{1}{t}\begin{bmatrix} 1 & -r \\ r & tt' - rr' \end{bmatrix} \tag{40}$$

Based on the above description, the relationship between the emission spectra of the two layers of material and the incident angle of the wave[13], the optical constants and the thickness of the material can be obtained in this paper as:

$$\gamma_{(l-1)} = \sum k_{(l-1)} d_{(l-1)} cos\theta_{(l-1)} \frac{t_1 t_2}{r_1 + r_2} \tag{41}$$

The relationship between the angle of incidence and the refractive index is expressed using the Snell's law of refraction[14], which is given in equation (5).

Therefore, the relationship between the emission spectra of the two-layer structure and the material properties is modeled as:

$$\gamma_{(l-1)} = \sum k_{(l-1)} d_{(l-1)} cos(arcsin\frac{n_{(l-1)} sin\theta_{(l-1)}}{n_l}) \frac{t_1 t_2}{r_1 + r_2} \tag{42}$$

Where$\gamma_{(l-1)}$is the emission spectrum of the two layers of material, and $d_{(l-1)}$is the thickness of each layer of material, and $\theta_{(l-1)}$ is the angle of incidence.

5.2.4. Modeling of multilayer structure emission spectra and material properties

Based on the modeling in part 5.2.3, the relationship between the emission spectra

of multilayer structures and material properties is obtained by generalizing Equation (42). Firstly, considering the phenomenon that absorption occurs between the multilayer materials in the process of radiation, and that this absorption leads to a more pronounced spectrum than the two-layer structure[15], the reflectance and transmittance at the interface of different materials are penalized in this article:

$$R = r_0^2 - \sigma\frac{r_1 t_1}{r_2 t_2} + \frac{|t_1 t_2 r_1|^2 e^{-4\frac{\sigma}{c}k_1 d_1}}{1 - |r_1 r_2|^2 e^{-4\frac{\sigma}{c}k_1 d_1}} \tag{43}$$

$$T = t_0^2 + \sigma\frac{r_1 r_2}{t_1 t_2} + \frac{|t_2|^2 e^{-2\frac{\sigma}{c}k_1 d_1}}{1 - |r_1 r_2|^2 e^{-4\frac{\sigma}{c}k_1 d_1}} \tag{44}$$

Where σ is the penalty factor introduced by the absorption loss of the multilayer material.

The relationship between the emission spectrum of a multilayer material and the angle of incidence of the wave, the optical constant, and the thickness of the material is also obtained from Maxwell's equations and the matrix transfer method as:

$$\gamma_{(l-1)} = \sum k_{(l-1)} d_{(l-1)} cos\theta_{(l-1)} \frac{t_1 t_2}{r_1 + r_2} + \sigma\left(\frac{r_1 r_2}{t_1 t_2} - \frac{r_1 t_1}{r_2 t_2}\right) \tag{45}$$

The relationship between the angle of incidence and the refractive index is expressed using the Snell's law of refraction, which is given in equation (5).

Therefore, the model of emission spectra of multilayer structures in relation to material properties is expressed as:

$$\gamma_{(l-1)} = \sum k_{(l-1)} d_{(l-1)} cos\left(arcsin\frac{n_{(l-1)} sin\theta_{(l-1)}}{n_l}\right) + \sigma\left(\frac{r_1 r_2}{t_1 t_2} - \frac{r_1 t_1}{r_2 t_2}\right) \tag{46}$$

Where $\gamma_{(l-1)}$ is the emission spectrum of the two layers of material, and $d_{(l-1)}$ is the thickness of each layer of material, and $\theta_{(l-1)}$ is the angle of incidence.

5.2.5. Analysis of results

In this paper, the equation mentioned above is calculated by MATLAB software for tungsten and silica with 50 nm thickness, i.e. $d_i = 50nm$, i=1,2, brought into Equation (46). The emission spectra of 50 nm thick tungsten and silica in the range of 0.3-50 μm are calculated by the relevant codes of the electromagnetic wave propagation equation and matrix transfer method as follows[16].

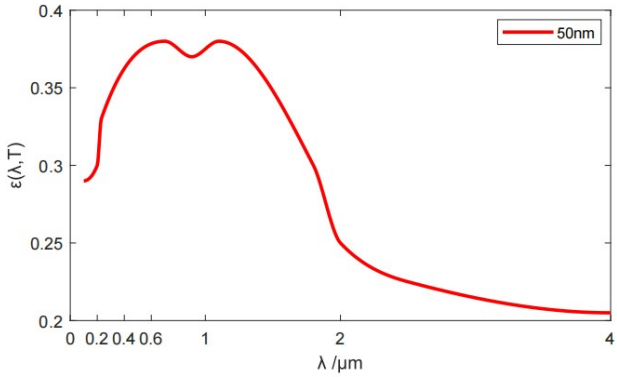

Figure 7: 50nm emission spectra of tungsten and silica

The model was tested by substituting values for different thicknesses of tungsten and silica into Equations and the following emission spectra were obtained.

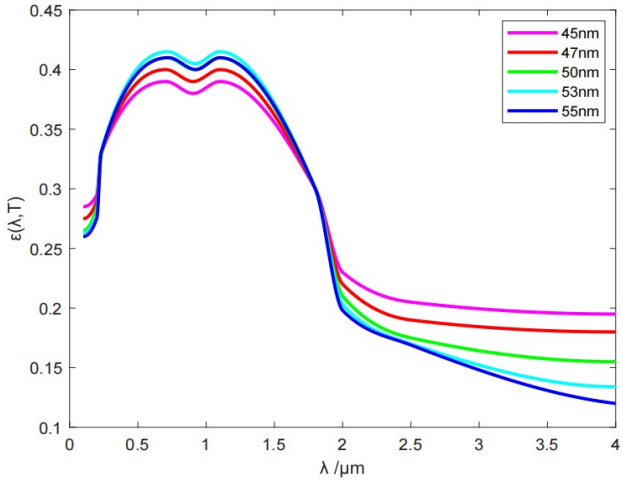

Figure 8: Emission spectra of tungsten and silica with different thicknesses

The figures show that the trends of emission spectra are similar for different thicknesses of tungsten and silica to some extent[17]. Therefore the model established for the emission spectra of multilayers with respect to material properties is considered to be correct.

5.3. Model and solution of problem three

In order to improve the spectral control of thermal emitters, the design of thermal emitters to emit in a narrow band form is nowadays becoming the current dominant approach. For the 26 materials given in this topic, the selection of each layer of a multilayer structured thermal emitter can make the number of candidate materials in the material search space enormous, making the optimal design of a multilayer structured thermal emitter complex and difficult[18]. To overcome the difficulties encountered above, this article introduces material informatics to solve the problem, which can effectively identify materials with preferred properties and greatly reduce the optimal solution sought in the search space. It is also possible to reduce the number of iterations in the process of solving the optimal solution by using Bayesian optimisation to co-opt the unknown function of the optimal material.

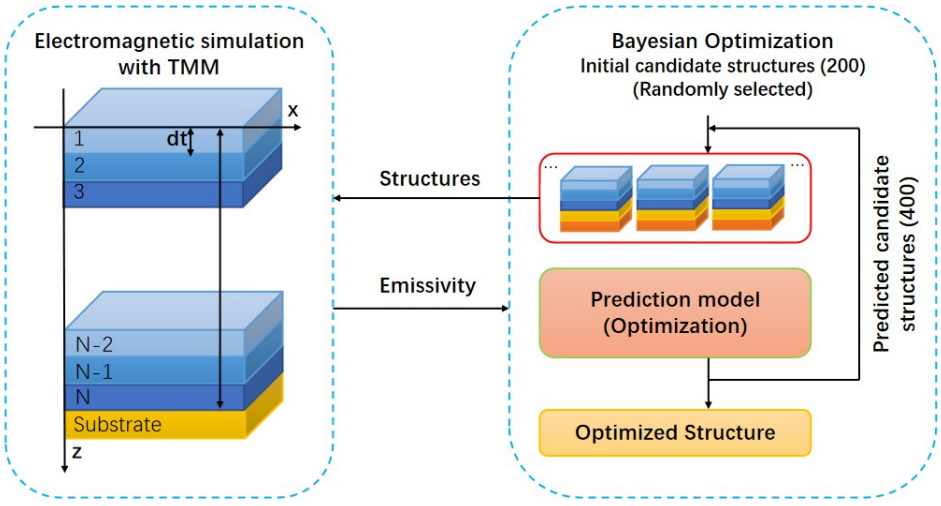

Figure 9: Bayesian optimization diagram

5.3.1. Optimal modeling of multilayered structural thermal emitters

For the optimal solution of the model of a multilayer structured thermal emitter, the optimal model of the multilayer structured thermal emitter is developed based on the relationship between the emission spectrum and the material properties of the multilayer structured thermal emitter in the second problem[19].

5.3.1.1. Objective function of a multilayer structured thermal emitter model

For the multilayer structural thermal radiation model in this question, the emission spectrum of the thermal emitter is used as the objective function of the model based on Problem 2 to find its maximum at a wavelength of 1.5 μm, the specific expression for which is:

$$max\ \gamma_{(l-1)} = \sum k_{(l-1)} d_{(l-1)} cos(arcsin\frac{n_{(l-1)} sin\theta_{(l-1)}}{n_l}) + \sigma(\frac{r_{l-1} r_{l+1}}{t_{l-1} t_{l+1}} - \frac{r_{l-1} t_{l-1}}{r_{l+1} t_{l+1}}) \quad (47)$$

Where $\gamma_{(l-1)}$ is the emission spectrum of the two layers of material, and $d_{(l-1)}$ is the thickness of each layer of material, $\theta_{(l-1)}$ is the angle of incidence, and the wavelength is in the range of 0.3-5 μm.

5.3.1.2. Multilayer structural heat emitter model constraints

A. Thickness constraints for multilayer structural thermal emitters

Considering that the radiation of each layer of material receives its thickness and that the thickness also indirectly affects the radiation of different layers of material, the following constraints are placed on the thickness of the thermal emitter based on the results obtained in the first and second questions.

$$42\text{nm} \le d_i \le 58nm \quad (48)$$

B. Refractive index constraints for multilayer structured thermal emitters

For the refractive index of a multilayer structured thermal emitter, considering the Snell's law of refraction, the model to be developed is constrained so that its refractive index r_i lies within the product of the Snell's coefficient and the cosine of the refraction angle of the upper and lower layers of the material, as expressed by:

$$\mathrm{n_{i-1}cos\theta_{i-1}} \le r_i \le \mathrm{n_{i+1}cos\theta_{i+1}} \quad (49)$$

C. Transmittance constraints for multilayer structural thermal emitters

For the transmittance of a multilayer structured thermal emitter, the transmittance values of the two adjacent layers of material can first be found according to the Snell's law. According to the loss phenomenon existing between multilayer structured radiators there is an expression for the transmittance constraint as:

$$\frac{2\mathrm{n_{i-1}cos\theta_{i-1}}}{\mathrm{n_{i-1}cos\theta_{i-1}} + \mathrm{n_{i+1}cos\theta_{i+1}}} \le t_i \le \frac{2\mathrm{n_{i+1}cos\theta_{i+1}}}{\mathrm{n_{i-1}cos\theta_{i-1}} + \mathrm{n_{i+1}cos\theta_{i+1}}} \quad (50)$$

D. Penalty term constraints for multilayer structural thermal emitters

For multilayer structural thermal emitters when electromagnetic interactions are carried out between them, the phenomenon of radiation loss during the transfer process occurs. Depending on the radiation losses occurring during the transfer process for the different layers of material, the following constraints apply.

$$\frac{\mathrm{k_l}}{\omega\varepsilon_i\varepsilon_{i+1}} \le \sigma \le \mathrm{w}\sqrt{\epsilon_i\mu_i\epsilon_{i+1}\mu_{i+1}} \quad (51)$$

E. Constraints on the number of layers of a multilayer structural thermal emitter

In order to simplify the complexity of the problem, this article places constraints on the number of layers l of a multilayer structural heat emitter to ensure that the number of layers is not too large.

$$6 \le l \le 14 \tag{52}$$

5.3.1.3. Modeling the optimal multilayer structured thermal emitter

In summary, the optimal multilayer structural thermal emitter model is developed in this paper and is shown below.

$$\text{Max}\,\gamma_{(l-1)} = \sum k_{(l-1)} d_{(l-1)} cos(arcsin\frac{n_{(l-1)}sin\theta_{(l-1)}}{n_l}) + \sigma(\frac{r_{l-1}r_{l+1}}{t_{l-1}t_{l+1}} - \frac{r_{l-1}t_{l-1}}{r_{l+1}t_{l+1}}) \tag{53}$$

$$\text{s.t.}\begin{cases} \frac{2n_{i-1}cos\theta_{i-1}}{n_{i-1}cos\theta_{i-1}+n_{i+1}cos\theta_{i+1}} \le t_i \le \frac{2n_{i+1}cos\theta_{i+1}}{n_{i-1}cos\theta_{i-1}+n_{i+1}cos\theta_{i+1}} \\ \frac{k_l}{\omega\varepsilon_i\epsilon_{i+1}} \le \sigma \le w\sqrt{\epsilon_i\mu_i\epsilon_{i+1}\mu_{i+1}} \\ n_{i-1}cos\theta_{i-1} \le r_i \le n_{i+1}cos\theta_{i+1} \\ 42nm \le d_i \le 58nm \\ 6 \le l \le 14 \end{cases}$$

This problem is solved by using a Bayesian optimisation method to find the number of layers, the material per layer and the thickness of each layer when it can reach its maximum value at 1.5 μm.

5.3.2. Solution of a multilayer structural thermal emitter model

In this paper, a Bayesian optimisation approach is adopted for the solution of the multilayer structural thermal radiator model. The core idea is to first generate an initial set of candidate solutions and then iterate over the candidate solutions to find the next point with the highest extreme confidence to add to the set. This step is repeated until the iteration is terminated[20]. Finally, the point that maximises the value of the function is found from these points as the solution to the problem.

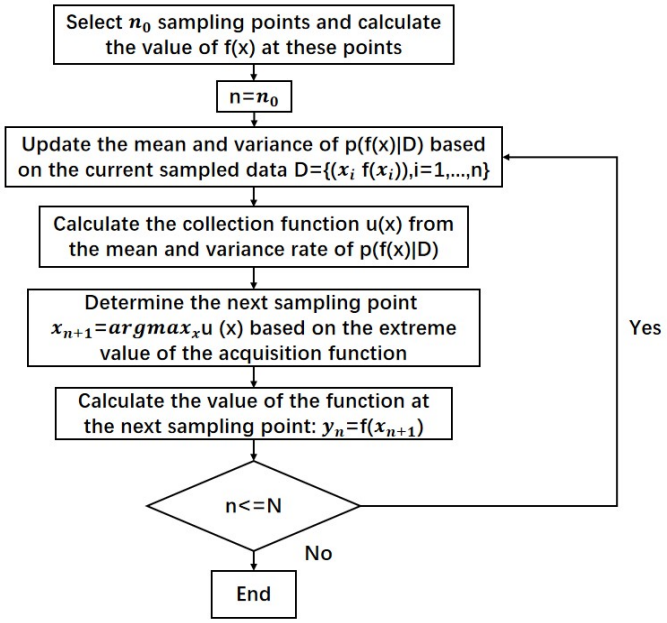

Figure 10: Bayesian optimization flow chart

The core of the Bayesian optimisation process consists of two main parts. The first is a Gaussian regression process, which calculates the mean and variance of the function values at each point. The second is the Gaussian acquisition process, which constructs the acquisition function based on the mean and variance of the number of layers, the type of material in each layer and the thickness of each layer obtained from the thermal radiator model, and is used to determine which points are acquired during the iterative Bayesian optimisation process.

A. Gaussian regression process

For the maximum value of the radiation required to solve this problem, which is related to the number of layers of material, the type of material in each layer, and the thickness of each layer, it can be simplified to:

$$\gamma_l = \gamma_l(\text{layer,type,thick}) \tag{53}$$

In the Bayesian optimization process, assume that there are already n points in the Bayesian candidate set, and when considering the value of the next search point x, x = (layer_i, type_i, thick_i), there is the formula:

$$\text{E}I_n(x) = E_n[[\gamma_l(x) - \gamma_l^*]^+] \tag{54}$$

In this article it is assumed that it obeys a normal distribution during the Gaussian regression process. The above E is therefore discretized and summed to represent the cumulative effect of the solution of the multilayer structural thermal radiator on the optimisation process in the earlier stages of the Bayesian optimisation process. This is specifically expressed as:

$$EI_n(x) = \sum [z - \gamma_l^*]^+ \frac{1}{\sqrt{2\pi}\sigma} e^{-\frac{(z-\mu)^2}{2\sigma^2}} \tag{55}$$

where z is the next search point and σ is the variance of the accumulated values of the multilayer structured thermal emitter during the optimization process.

B. Gaussian acquisition process

For the Gaussian acquisition process, after comparing the value of the radiation at the search point with the value of the radiation in the set of candidate solutions, if the value at the search point is greater than the value in the set of candidate solutions, the search value is added to the set of candidate solutions, expressed by the following equation.

$$\begin{aligned} &if \quad \gamma_l(layer_i, type_i, thick_i) \geq \gamma_l^* \\ &\quad (layer_i, type_i, thick_i) \quad join\ in\ Candidate \\ &\quad \text{set} \end{aligned} \tag{56}$$

The values of the newly added points are corrected as follows.

$$\gamma_l^{'} = \gamma_l(layer_i, type_i, thick_i) - \gamma_l^* \tag{57}$$

The next sampled point is found by correcting the value of the newly added point according to the expected value in the set of candidate solutions, which is expressed as follows:

$$\begin{aligned} &(layer_i, type_i, thick_i) = \\ &argmaxEI_n(layer_i, type_i, thick_i) \end{aligned} \tag{58}$$

5.3.3. Analysis of results

By modelling the multilayer structured thermal emitter as described above and solving it using Bayesian optimization, the optimal number of layers, the material of each layer and the thickness of each layer for a sharp and high thermal radiation value at 1.5 μm is derived as shown in the table below.

Table 2: Results of Model Solving

Optimal solution results	layers	Material per layer (top-down)	Thickness of each layer (μm)	Q-factor	Thermal radiation value (1.5μm)
result 1	9	Ge,Y2O3,Ge,Y2O3,Ge, Y2O3,Ge,SiO2,W	3.85	192	0.41
result 2	12	Ge,SiO2,Ge,Y2O3,Ge,Y2O3, Ge,SiO2,Ge, SiO2,ZnO,W	3.78	191	0.39
result 3	10	Ge,SiO2,Ge,Y2O3,Ge,Y2O3, Ge,SiO2,ZnO,W	3.81	190	0.42
result 4	8	Ge,SiO2,Ge,SiO2,Ge, SiO2,Y2O3,W	3.87	194	0.38

For each layer of material, the assembly of the thermal emitter is carried out in the form of a laminated crossover, as shown in the following figure.

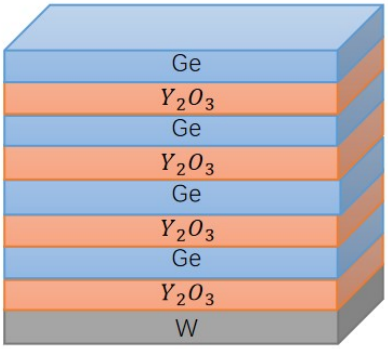

Figure 11: Structure diagram of heat emitter

And for the calculated results, the emission spectra are shown below.

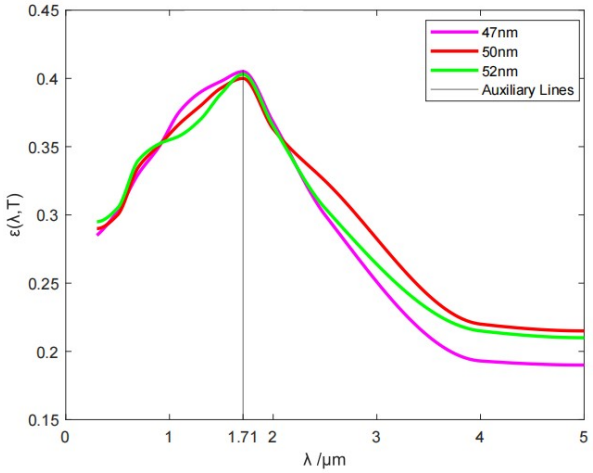

Figure 12: Emission spectrogram

5.4. Model and solution of problem four

This problem is to design a multilayer structured heat emitter for GaSb cells. According to Problem 3, the multilayer structured heat emitter is firstly modelled and its objective function is modified accordingly, and then the established heat emitter model is solved by a particle swarm optimisation algorithm to obtain the design parameters of the multilayer heat emitter structure. Finally, a model check is carried out to verify the correctness of the model by adding the external quantum efficiency (EQE).

5.4.1. Optimal modeling of multilayer structural thermal emitters

For the optimal solution of the multilayer structured thermal emitter model, the optimal model of the multilayer structured thermal emitter is established based on the relationship between the emission spectrum and the material properties of the multilayer structured thermal emitter in the second question.

5.4.1.1. Multilayer structural heat emitter model objective function

For this problem, the emission spectrum of the thermal emitter is used as the objective function of the model based on Problem 2 to find its maximum at a wavelength of 1.71 μm, which is specified by the expression:

$$\max\ \gamma_{(l-1)} = \sum k_{(l-1)} d_{(l-1)} cos(arcsin \frac{n_{(l-1)} sin\theta_{(l-1)}}{n_l}) + \sigma(\frac{r_{l-1} r_{l+1}}{t_{l-1} t_{l+1}} - \frac{r_{l-1} t_{l-1}}{r_{l+1} t_{l+1}}) \quad (59)$$

Where $\gamma_{(l-1)}$ is the emission spectrum of the two layers of material, $d_{(l-1)}$is the thickness of each layer of material, $\theta_{(l-1)}$ is the angle of incidence, and the wavelength is in the range of 0.3-5 μm.

5.4.1.2. constraints of the multilayer structural thermal emitter model

For the constraints of the model of the multilayer structural thermal emitter in this question, the constraints of the model proposed in the Problem 3 can be referred to and will not be elaborated here.

5.4.1.3. Modeling of optimal multilayer structural thermal emitters

Above all, the optimal multilayer structural thermal emitter model is developed and shown below.

$$\max \gamma_{(l-1)} = \sum k_{(l-1)} d_{(l-1)} cos(arcsin \frac{n_{(l-1)} sin\theta_{(l-1)}}{n_l}) + \sigma(\frac{r_{l-1} r_{l+1}}{t_{l-1} t_{l+1}} - \frac{r_{l-1} t_{l-1}}{r_{l+1} t_{l+1}}) \quad (60)$$

$$\text{s.t.} \begin{cases} \frac{2n_{i-1}\cos\theta_{i-1}}{n_{i-1}\cos\theta_{i-1}+n_{i+1}\cos\theta_{i+1}} \le t_i \le \frac{2n_{i+1}\cos\theta_{i+1}}{n_{i-1}\cos\theta_{i-1}+n_{i+1}\cos\theta_{i+1}} \\ \frac{k_l}{\omega\varepsilon_i\varepsilon_{i+1}} \le \sigma \le w\sqrt{\epsilon_i\mu_i\epsilon_{i+1}\mu_{i+1}} \\ n_{i-1}\cos\theta_{i-1} \le r_i \le n_{i+1}\cos\theta_{i+1} \\ 42nm \le d_i \le 58nm \\ 6 \le l \le 14 \end{cases}$$

In this paper, a particle swarm algorithm was presented to find the number of layers, the material per layer and the thickness of each layer when it can reach its maximum value at 1.71 μm.

5.4.2. Solving a multilayer structural heat emitter model

For the model of a multilayer structural heat emitter, this paper uses a particle swarm algorithm to solve it. The core idea is to first assign initial random positions and initial random velocities to all particles in the solution space, and then advance each particle in turn according to its velocity, the known optimal global solution position in the problem space and the known optimal position of the particle. As the swarm of particles continues to evolve, all points in the search space will cluster around one or more optimal points, and in this way the optimal solution to the problem is obtained.

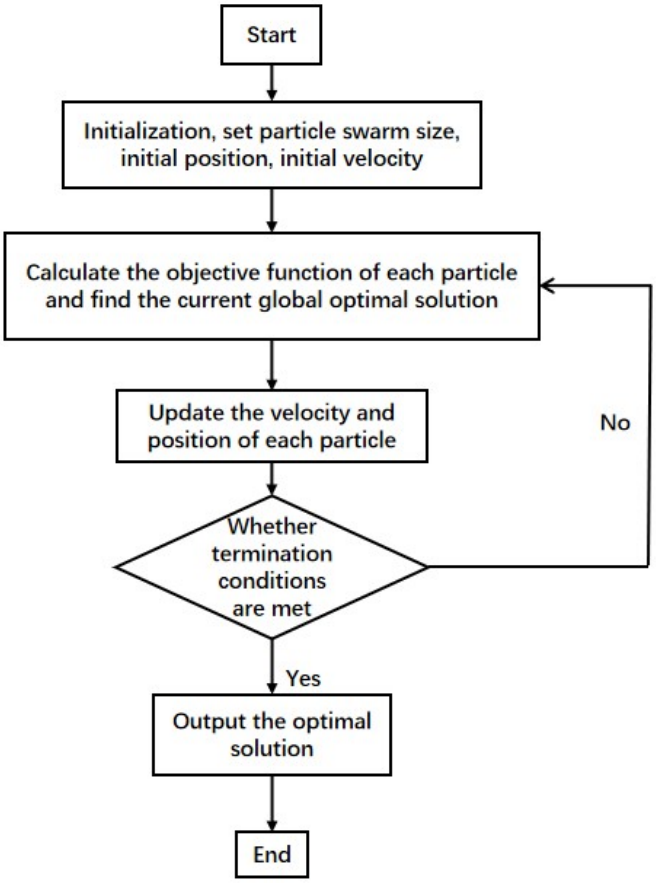

Figure 13: Flow chart of the particle swarm algorithm

For the particles in the particle swarm, this paper treats ($\text{layer}_i, \text{type}_i, \text{thick}_i$) is considered as a point in the solution space and its velocity is decomposed into three directions that are orthogonal to each other, while being represented by the number of layers, the type of multilayer material and the thickness of the multilayer material, respectively.

$$V_i(layer_i, type_i, thick_i) = C_1\, random(0,1)(P - V_i) + C_2 random(0,1)(P - V_i') \tag{61}$$

Of which C_1 ,C_2 are constants and P is the current global optimal solution.
The particle swarm pseudocode is shown below.

The PSO algorithm

Initialize particle swarm ;
Do
  for each particle
    Calculate its adaptation degree ;
    if (adaptation better than particle historical best)
      Update the historical best question Pi with Xi ;
  end
  Select the best particle in the current particle swarm ;
  if (the current best particle is better than the group's historical best particle)
    Update Pg with the best particle of the current swarm ;
  for each particle
    Update the particle velocity by equation (1) ;
    Update the particle position by equation (2) ;
  end
While maximum number of iterations not reached or minimum error not reached

5.4.3. Results analysis

The model of the multi-layer structure heat radiator is established and solved by using particle swarm optimization algorithm. The optimal number of layers, the material of each layer and the thickness of each layer at 1.71 micron are obtained.Its values are shown in the following table:

Table 3: Results of Model Solving

Optimal solution results	layers	Material per layer (top-down)	Thickness of each layer (μm)	Thermal radiation value (1.71μm)
result 1	9	Y2O3,Ge,Y2O3,Ge,Y2O3, Ge,SiO2,Ge,GaSb	3.75	0.37
result 2	12	SiO2,Ge,Y2O3,Ge,Y2O3,Ge, SiO2,Ge,SiO2,Ge,ZnO,GaSb	3.68	0.39
result 3	10	SiO2,Ge,Y2O3,Ge,Y2O3,Ge, SiO2,Ge,ZnO,GaSb	3.71	0.38

For each layer of material, the assembly of the thermal emitter is carried out in the form of a laminated crossover, as shown in the following figure.

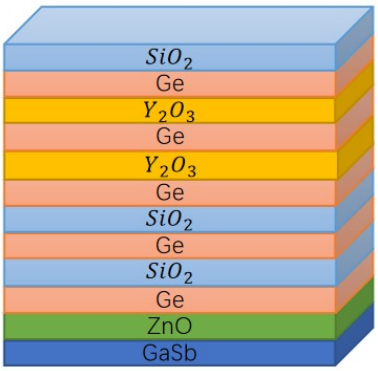

Figure 14: Thermal emitter structure

And for the calculated results, the emission spectra are shown below.

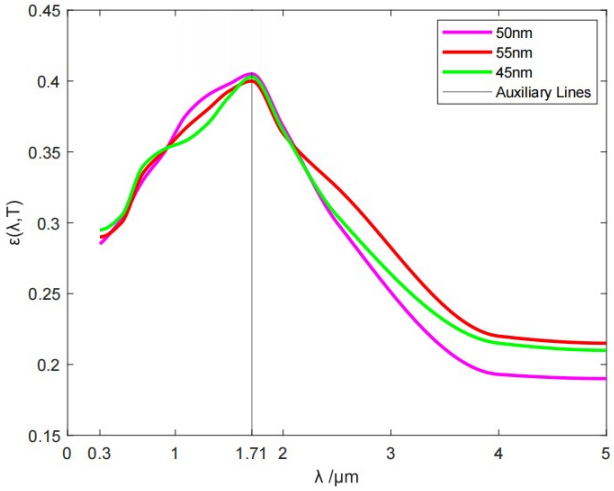

Figure 15: Emission spectrum of thermal emitter

5.4.4. Model testing

For the multilayer structured thermal emitter model developed above, this paper performs a sensitivity check on it by adding constraints to the model, with the following external quantum efficiency constraints on the model:

$$50\% \leq \text{EQE} = \frac{N_{collect}}{N_{total}} \leq 80\% \tag{61}$$

Besides, considering that the multilayer thermal emitter achieves the highest possible thermoelectric conversion efficiency, the objective function of the model is modified accordingly with the following equations:

$$\max\ \gamma_{(l-1)} = \sum k_{(l-1)} d_{(l-1)} cos(arcsin \frac{n_{(l-1)} sin\theta_{(l-1)}}{n_l}) + \sigma(\frac{r_{l-1} r_{l+1}}{t_{l-1} t_{l+1}} - \frac{r_{l-1} t_{l-1}}{r_{l+1} t_{l+1}}) \tag{62}$$

$$\max \eta = \frac{t_l - t_{l-1}}{t_l}(\sqrt{1 + \bar{t}Z} - 1) \tag{63}$$

In summary, there are multilayer structural thermal emitters modeled as follows.

$$\max\ \gamma_{(l-1)} = \sum k_{(l-1)} d_{(l-1)} cos(arcsin \frac{n_{(l-1)} sin\theta_{(l-1)}}{n_l}) + \sigma(\frac{r_{l-1} r_{l+1}}{t_{l-1} t_{l+1}} - \frac{r_{l-1} t_{l-1}}{r_{l+1} t_{l+1}}) \tag{64}$$

$$\max \eta = \frac{t_l - t_{l-1}}{t_l}(\sqrt{1 + \bar{t}Z} - 1) \tag{65}$$

$$\text{s.t.} \begin{cases} \frac{2n_{i-1}\cos\theta_{i-1}}{n_{i-1}\cos\theta_{i-1} + n_{i+1}\cos\theta_{i+1}} \leq t_i \leq \frac{2n_{i+1}\cos\theta_{i+1}}{n_{i-1}\cos\theta_{i-1} + n_{i+1}\cos\theta_{i+1}} \\ \frac{k_l}{\omega\varepsilon_i\varepsilon_{i+1}} \leq \sigma \leq w\sqrt{\epsilon_i\mu_i\epsilon_{i+1}\mu_{i+1}} \\ n_{i-1}\cos\theta_{i-1} \leq r_i \leq n_{i+1}\cos\theta_{i+1} \\ 50\% \leq \text{EQE} = \frac{N_{collect}}{N_{total}} \leq 80\% \\ 42\text{nm} \leq d_i \leq 58nm \\ 6 \leq l \leq 14 \end{cases}$$

The number of layers, the material of each layer and the thickness of each layer of the emitter with optimal values at 1.71 μm were derived by solving with the particle swarm algorithm. The values are shown in the following table.

Table4: Model solution results

Optimal solution results	layers	Material per layer (top-down)	Thickness of each layer (μm)	Thermal radiation value (1.71μm)
result 1	9	Y2O3,Ge,Y2O3,Ge,Y2O3,Ge,SiO2,Ge,GaSb	3.75	0.37
result 2	11	SiO2,Ge,Y2O3,Ge,Y2O3,Ge,Y2O3,SiO2,Ge,ZnO,GaSb	3.78	0.39
result 3	10	SiO2,Ge,Y2O3,Ge,Y2O3,Ge,SiO2,Ge,ZnO,GaSb	3.71	0.38

For each layer of material, the assembly of the emitter is carried out in the form of a laminated crossover, as shown in the following figure.

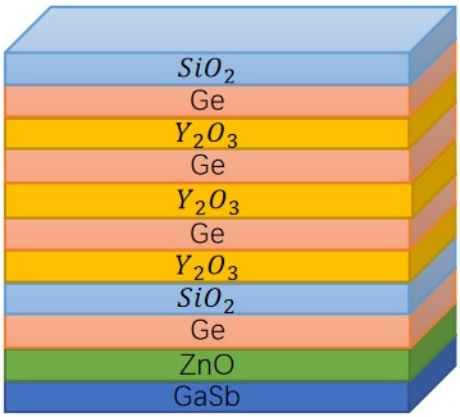

Figure 16: Thermal emitter structure

Finally, for the calculated results, the emission spectra are shown below.

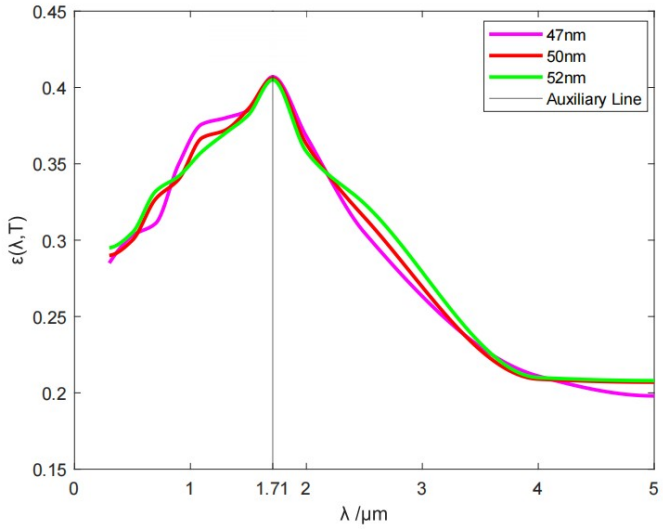

Figure 17: optical emission spectrometer

After adjusting the model while solving for the optimal values, the results are found to be within 7.2% error from the results before the adjustment. Consequently, it is reasonable to assume that the model developed in this question is correct.

6. model evaluation

6.1. Advantages

a. Particle swarm optimization algorithm has fast convergence speed, simple algorithm and friendly to optimization function.
b. Bayesian optimization with fewer iterations, faster speed and robust to nonconvex problems
c. Matrix transfer method is flexible in application. The transfer parameters in the system are solved by matrix multiplication.

6.2. Shortcomings

a. For multiple local extreme points, it is easy to fall into local extreme points, and the correct results are not obtained.
b. Bayesian optimization is not easy to find the global optimal solution, and it consumes a lot of resources and time.
c. The analysis of matrix transfer method is complex and requires a deeper understanding of the problem

6.3. Outlook

In this paper, single-layer emission spectrum and material properties model and multi-layer emission spectrum and material properties model are established. However, the selection of model parameters and the evaluation of objective function are not perfect, and the influence of various environmental factors in general is not considered. After the competition, it is intended to improve and optimize the model in this article and add the relevant content of machine learning to make the final design parameters of the thermal transmitter more reasonable and make the target value of the optimization function more accurate.

Reference

[1] Fan, S. Thermal photonics and energy applications. Joule 2017, 1(2), 264−273.

[2] Cui, L. J.; Jeong, W.; Fernandez-Hurtado, C.; Feist, J.; GarciaVidal, F. J.; Cuevas, J. C.; Meyhofer, E.; Reddy, P. Study of radiativeheat transfer in Angstrom- and nanometre-sized gaps. Nat. Commun.2017, 8, 14479.

[3]. P. Yeh, Optical Waves in Layered Media Wiley, New York,1988, p. 102.

[4]. Z. Knittl, Optics of Thin Films Wiley, London, 1976, p. 41.

[5]. G. K. Hubler, P. R. Malmberg, C. N. Waddell, W. G. Spitzer,and J. E. Fredrickson, in Ion Implantation for Materials Processing, F. A. Smidt, ed.Noyes Data, Park Ridge, N.J., 1983,p. 195–218.

[6]. W. Tennant and J. Cape, "Study of the dielectric function ofPbSnTe epitaxial film by far-infrared reflectivity," Phys. Rev. B13, 2540–25471976.

[7]. C. C. Katsidis, D. I. Siapkas, W. Skorupa, N. Hatzopoulos, andD. Panknin, Proceedings of the 10th International Conferenceon Ion Implantation Technology Elsevier, Amsterdam, 1995,p. 959–962.

[8]. C. C. Katsidis and D. I. Siapkas, in Proceedings of NATO ASIon Application ofParticle and Laser Beams in Materials Technology, P. Misaelides, ed.Kluwer Academic, Dordrecht, 1995,p. 603–612.

[9]. C. C. Katsidis, D. I. Siapkas, D. Panknin, N. Hatzopoulos, andW. Skorupa, "Optical characterization of doped Simox structures using FTIR spectroscopy, " Microelectron. Eng. 28, 439–442 1995.

[10]. N. Hatzopoulos, D. I. Siapkas, and P. L. F. Hemment, "Oxidegrowth, refractive index, and composition depth profiles ofstructures formed by 2 MeV oxygen implantation into silicon,"J. Appl. Phys. 77, 577–586 1995 .

[11]. D. I. Siapkas, N. Hatzopoulos, C. C. Katsidis, T. Zorba, C. L.Mitsas, and P. L. F. Hemment, "Structural and compositionalcharacterization of high energy separation by implantation ofoxygen structures using infrared spectroscopy," J. Electrochem. Soc. 143, 3019–3032 1996.

[12]. N. Hatzopoulos, D. I. Siapkas, P. L. F. Hemment, and W.Skorupa, "Formation and characterization of novel Si SiO2multilayer structures by oxygen ion implantation into silicon,"J. Appl. Phys. 80, 4960–49701996.

[13]. N. Hatzopoulos, D. I. Siapkas, and P. L. F. Hemment, "Opticalinvestigation of structures formed by 2MeV oxygen implantation into silicon," Thin Solid Films 289, 90–94

[14]. C. L. Mitsas and D. I. Siapkas, " Generalized matrix method foranalysis of coherent and incoherent reflectance and transmittance of multiplayer structures with rough surfaces, interfaces, and finite substrates," Appl. Opt. 34, 1678–1683

[15]. G. Lubberts, B. C. Burkey, F. Moser, and E. A. Trabka, "Optical properties of phosphorous-doped polycrystalline siliconlayers," J. Appl. Phys. 52, 6870–6878

[16]. I. Fillinski, "The effects of sample imperfections on opticalspectra," Phys. Status Solidi 49, 577–588

[17]. J. Szczyrbowski and A. Czapla, "Optical absorption in d.c.sputtered InAs films," Thin Solid Films 46, 127–137

[18]. J. Pawlikovski, "Comments on the determination of the absorption coefficient of thin semiconductor films," Thin SolidFilms 127, 29–38

[19]. H. E. Bennett, and J. O. Porteus, " Relation between surfaceroughness and specular reflectance at normal incidence," J.Opt. Soc. Am. 51, 123–129

[20]. A. Tikhonravov, M. Trubetskov, B. Sullivan, and J. Dobrowolski, "Influence of small inhomogeneities on the spectral characteristics of single thin films," Appl. Opt.36, 7188–7198

Appendix

code1:bayesian-optimization

```
def    rf_cv(n_estimators,    min_samples_split,    max_features,
max_depth):
   val = cross_val_score(
      RandomForestClassifier(n_estimators=int(n_estimators),
         min_samples_split=int(min_samples_split),
         max_features=min(max_features, 0.999), # float
         max_depth=int(max_depth),
         random_state=2
      ),
      x, y, scoring='roc_auc', cv=5
   ).mean()
   return val
rf_bo = BayesianOptimization(
      rf_cv,
      {'n_estimators': (10, 250),
      'min_samples_split': (2, 25),
      'max_features': (0.1, 0.999),
      'max_depth': (5, 15)}
   )
```

code2:particle swarm

```
clc;
clear all;
for i=1:sizepop
   pop(i,:)=popmax*rands(1,D);
   V(i,:)=Vmax*rands(1,D);
```

```
    fitness(i)=Griewank(pop(i,:));
end
for i=1:maxg
    for j=1:sizepop
        w=0.8;

V(j,:)=w*V(j,:)+c1*rand*(pBest(j,:)-pop(j,:))+c2*rand*(gBest-pop
(j,:));


        V(j,find(V(j,:)>Vmax))=Vmax;
        V(j,find(V(j,:)<Vmin))=Vmin;


        pop(j,:)=pop(j,:)+V(j,:);


        pop(j,find(pop(j,:)>popmax))=popmax;
        pop(j,find(pop(j,:)<popmin))=popmin;


        fitness(j)=Griewank(pop(j,:));


        if fitness(j)<fitnesspbest(j)
            pBest(j,:)=pop(j,:);
            fitnesspbest(j)=fitness(j);
        end


        if fitness(j)<fitnessgbest
            gBest=pop(j,:);
            fitnessgbest=fitness(j);
        end
    end
    result(i)=fitnessgbest;
```

```
end
```

code3: wave function

```
t=0:0.00001:3-0.00001;
f0=5;
fe=100;
x=chirp(mod(t,1),f0,1,fe);
ft=f0+(fe-f0)*mod(t,1);
subplot(3,1,2);plot(t,ft);title('');xlabel('');ylabel('(Hz)');
t=0:0.00001:3-0.00001;
f0=5;
fe=100;
x=chirp(mod(t,1),f0,1,fe);
subplot(3,1,1);plot(t,x);title('');xlabel('(s)');ylabel('(V)');

ft=f0+(fe-f0)*mod(t,1);
subplot(3,1,2);plot(t,ft);title('');xlabel('(s)');ylabel('(Hz)')
;

t=0:0.00001:1;
x=chirp(t,f0,1,fe);
C1=fft(x);
cxf=abs(C1);
cxf=cxf/max(cxf);
% subplot(3,1,3);plot(f(1:N/2),cxf(1:N/2)); axis([0 150 0 1]);
subplot(3,1,3);plot(cxf); axis([0 150 0 1]);
title('');xlabel('(Hz)');ylabel('');
```